

## **Supplemental Materials and Methods**

### ***Chromatin immunoprecipitation assays and genome-wide location analysis***

ChIP-on-chip data acquisition and analysis were performed based on the whole-chip error model (Acosta-Alvear et al, 2007; Cao et al, 2006), and MyoD1 binding to genomic regions was determined using the following criteria: A genomic region is considered bound if the enrichment  $p$ -value for the region (probe neighborhood) is less than or equal to 0.005 *and* the enrichment  $p$ -value for the individual probe is equal to or less than 0.001 (Cao et al, 2006; Lee et al, 2006). In addition, individual probes were considered bound if the normalized binding ratio for IP/WCE (where WCE is the reference whole cell extract DNA) was above a cut-off threshold of 2.5 as described in similar experiments using the same antibody (Blais et al, 2005). These criteria were chosen for the determination of transcription factor-DNA binding events because they have proven to be reliable, with an acceptable false positive error rate in similar experiments (Blais et al, 2005; Cao et al, 2006; Lee et al, 2006). Individual binding events of interest were verified in conventional ChIP analyses.. To illustrate the transcription factor-DNA binding events of interest, neighboring probes in the promoter regions of target genes were mapped to the UCSC Genome Browser mm8 assembly genome and the relative fold-enrichment afforded by the IP procedure for each one of these probes was plotted as a function of their genomic coordinates. Each one of the individual binding events of interest was verified in conventional ChIP analyses. Sequences for the PCR primers utilized are available on request. MyoD1 polyclonal antibody was used (clone M-318, Santa Cruz Biotechnology).

### ***RNA interference***

RNAi was performed with custom siRNA duplexes (Dharmacon) transfected with

siMPORTER (Millipore) at a concentration of 100 nM each. Sequences are available upon request.

### ***Immunoblotting***

Samples were lysed in RIPA buffer (150 mM NaCl, 1% NP-40, 0.5% sodium deoxycholate, 0.1% SDS, 50 mM Tris-HCl pH 8.0, and protease inhibitors), separated by SDS-PAGE, transferred onto nitrocellulose and probed with anti-TBP (SI-1)(Santa Cruz Biotechnology), anti-NF $\kappa$ B p65 (Cell Signaling Technology), or anti- $\alpha$ -tubulin antibodies (Sigma). Other antibodies included: anti-NEMO (NCI preclinical repository) and Medical and Biological Laboratories Co. (MBL, clone EA2-6), anti-Ub (clone FK2, Biomol International), and anti-pRB (BD Pharmingen). Quantification was performed using Quantity One (Biorad) and ImageJ (NIH).

### ***Immunofluorescence, BrdU incorporation, and image acquisition***

MHC staining and BrdU labeling and detection were performed as described (Blais et al, 2005), except that the BrdU labeling time was shortened to 20 min. Fluorescence and bright field micrographs were acquired with an Axiovert 200M fluorescence microscope (Zeiss) and Metamorph (MDS Analytical Technologies). MCH pixel density was calculated by counting the number of pixels in the red (MHC) and blue (DAPI) channels using Metamorph (MDS Analytical Technologies). The median pixel density for MHC was normalized against that of DAPI for each of three fields.

### ***RT-PCR and RT-qPCR analysis***

Semi-quantitative reverse-transcription polymerase chain reaction (RT-PCR) was performed as described (Blais et al, 2005). Quantitative RT-PCR (qRT-PCR) was

performed using SYBR green with a BioRad iCycler (BioRad Laboratories). Sequences for the PCR primers utilized are available on request

### ***Cellular fractionation***

Cytoplasmic and nuclear extracts were prepared as described (Asp et al, 2009). 100 µg of extract were separated on 15% SDS-PAGE, transferred onto nitrocellulose, and subjected to immunoblotting.

### ***Retroviral transduction***

Ecotropic recombinant retroviruses were produced in Phoenix cells as described (Asp et al, 2009).

### ***Purification of Traf7-associated proteins and mass spectrometry***

Confluent (T0) C2C12 cells stably expressing Flag-HA-Traf7 were lysed in NE buffer (10 mM HEPES pH 8, 250 mM KCl, 0.1% NP-40, 0.1 mM EDTA, 10% glycerol and protease/phosphatase inhibitors). 40 mg of lysate were subjected to tandem immuno-affinity purification with FLAG-M2 agarose beads (Sigma), eluted with 100 µM 3xFLAG peptide), and purified using a MonoQ column (GE Healthcare), which was eluted with a linear gradient from 50 mM to 750 mM KCl followed by a step elution with 1 M KCl in BC Buffer (20 mM Tris, pH 7.6, 0.2 mM EDTA, 10 mM β-mercaptoethanol, 10% glycerol, and protease inhibitors). The purified complexes were resolved by SDS-PAGE, and the two resulting FLAG-HA-Traf7 peaks (between 350 and 570 mM KCl, assessed by immunoblotting), were processed separately. Co-eluting proteins from each peak were separated by SDS-PAGE, excised, trypsinized, and subjected to microcapillary liquid chromatography coupled to tandem mass spectrometry as described previously (Spektor et al, 2007).

## Supplemental Figure Legends

### Table S1. MyoD1 targets associated with ubiquitin-related processes

#### Figure S1. MyoD1 regulates genes associated with Ub-related processes.

Enrichment profile for selected genomic loci bound by MyoD1. Relative fold-enrichment ratios for MyoD1 in the proximal promoter regions of selected targets are shown. *Rapsn*, *Chrna1*, positive controls (Liu et al, 2000; Ohno et al, 2003).

**Figure S2. Effect of ablating Traf7 on myogenesis.** (A) IF analysis of MHC expression in C2C12 myoblasts depleted of *Traf7* that were induced to differentiate (T=48). RNAi of *Traf7* was performed using four individual silencing RNA duplexes. Bars: 40  $\mu\text{m}$  for 10x magnification. (B) RT-PCR validation of *Traf7* siRNAs used in (A) at T=48. NS, non-specific siRNA; *Rps26*, input and loading control.

**Figure S3. Traf7 control of cell cycle exit.** (A) Rows 1-3: IF analysis of MHC expression in C2C12 myoblasts depleted of *Traf7* (i*Traf7*) and induced to differentiate for 24, 48, or 96 hours. Last row: MHC expression in confluent myoblasts depleted of *Traf7* and induced to differentiate in the presence of growth medium (GM) for 24 hours (Yoshiko et al, 2002). Numbers in the lower right corner indicate normalized MHC signal (MHC/DAPI) for the i*Traf7* cultures versus that of the non-specific control. For each time point, mean myotube length and number were averaged over 3 different fields. T=24 hours (average of 245 myotubes, length 123.4  $\mu\text{m}$ , for i*Traf7* vs. 184 myotubes, length 89.17  $\mu\text{m}$ , for NS per field); T=48 hours (149 myotubes, length 311.39  $\mu\text{m}$ , for i*Traf7* vs. 114 myotubes, length 110.33  $\mu\text{m}$ , for NS per field); T=96 hours (104

myotubes, length 422  $\mu\text{m}$ , for iTraf7 vs. 95 myotubes, length 399.7  $\mu\text{m}$ , for NS per field). **(B)** IF analysis of MHC expression in Traf7-depleted, sub-confluent, growing myoblasts (T=48). Right panel: Average fold-enrichment of MHC-positive C2C12 cells per field (n=6 fields). **(C)** IF analysis of FLAG-Traf7 (green) and MHC (red) expression in C2C12 myoblasts transiently transfected with FLAG-Traf7 (upper panel) or FLAG vector (bottom), and differentiated for 48h. Scale bars: 40  $\mu\text{m}$  for 10x magnification. Mean of 97 myotubes of 33.8  $\mu\text{m}$  length for FLAG-Traf7 vs. 173 myotubes of 52  $\mu\text{m}$  for vector alone per field (n=5 fields). Normalized MHC/DAPI ratio for FLAG-Traf7 versus vector alone control is shown at lower right of upper MHC panel.

**Figure S4. Ectopic expression of Traf7 does not provoke apoptosis.**

**(A)** Trypan blue staining. C2C12 cells were transfected with the vector alone control or with FLAG-Traf7, stained 48 hrs post-transfection (48hrsPT or T0) with Trypan blue and counted. Positive controls included 10  $\mu\text{M}$  MG132 treatment for 24h and 200  $\mu\text{M}$  etoposide treatment for 16h, both of which induced robust cell death (Lauricella et al, 2003; Jullig et al, 2006). *(Left)* The percentage of Trypan Blue stained cells is shown. Error bars represent SEM for n=3 fields. *(Right)* RT-PCR analysis of transfected and treated cells. We also differentiated cells for an additional 48 hours (96h PT) and saw no change in the ratio of viable to non-viable cells as compared to controls (not shown). **(B)** Cleaved caspase 3 was detected by immunofluorescence. Transfections were performed as in (A). *(Left)* Quantitation of IF analysis. C2C12 cells stained with antibodies that specifically detect cleaved caspase 3 (Cell Signaling, antibody #9661). MG132 treatment 10  $\mu\text{M}$ , 24hrs. Error bars represent SEM of n=3 fields. *(Right, top)* RT-PCR analysis of transfected or treated cells. *(Right, bottom)* Immunoblot analysis of transfected cells. **(C)** FACS analysis of cells ectopically expressing Traf7. *(Top)* C2C12 cells were co-transfected with control vector or FLAG-Traf7 together with a GFP plasmid. 48hrs later, cells were harvested, stained with propidium iodide, and FACS analysis was performed

on cells gated for GFP fluorescence. Propidium iodide fluorescence is depicted as PE. Apoptotic population is presented as a sub-G1 population. Percentage of cells in sub-G1, G1, S, and G2/M is in the graph. (*Bottom*) RT-PCR analysis of transfected cells.

**Figure S5. Ectopic expression of Traf7 delays myogenic differentiation**

(A) IF analysis of MHC expression (red channel) in C2C12 myoblasts transiently transfected with FLAG-Traf7 and FLAG- $\Delta$ 89 Traf7 (RING domain mutant) at T=48. Numbers (top row) indicate the normalized ratio of MHC fluorescence for FLAG-Traf7 and FLAG- $\Delta$ 89 Traf7 transfected cultures versus that of empty vector controls. Scale bar, 30  $\mu$ m for 20x magnification. (B) IF analysis of FLAG-Traf7 (top and middle panel) and FLAG- $\Delta$ 89 Traf7 localization (third row) in transiently transfected C2C12 myoblasts induced to differentiate for 48 hours shows non-identical, but overlapping, localization in the cytoplasm. Top panel: 20 $\times$  magnification. Second and third panel: 63 $\times$  magnification.

**Figure S6. Acute depletion of Traf7 promotes premature myogenic differentiation**

**by modulating cell cycle gene expression.** (A) qRT-PCR analysis of cell cycle genes after Traf7 RNAi. The analysis was performed on confluent cultures prior to induction of differentiation. Relative expression fold-changes iTraf7 vs NS siRNA duplex are shown for selected genes. Error bars: SEM derived from three independent experiments. \* indicates a *p*-value < 0.1, \*\* indicates a *p*-value < 0.05, and \*\*\* indicates a *p*-value < 0.01 using Student's one-tail paired *t*-test. All values were normalized against a loading control, *Rps26*. (B) qRT-PCR analysis of expression of selected cell cycle genes in

growing C2C12 myoblasts depleted of Traf7. Fold-changes in expression of selected genes, error bars, and normalization as in panel A. (C) Quantification of BrdU incorporation in Traf7-depleted differentiating C2C12 cultures. Error bars and normalization as in panel A.

**Figure S7. Traf7 specifically interacts with NEMO and enhances NEMO ubiquitylation in muscle cells.** (A) Diagram illustrating purification strategy used to isolate Traf7-associated proteins for proteomic analysis. Purification of Traf7-associated proteins from C2C12 cells stably expressing FLAG-Traf7. FLAG-Traf7 eluted in two different peaks (0.35M KCl and 0.57M KCl). Both fractions were subjected to mass spectrometry, and NEMO was identified in the 0.35 M KCl peak. (B) NEMO ubiquitylation is not substantially altered by MG132. Immunoblot to detect ubiquitylation of NEMO in lysates of confluent C2C12 myoblasts that were transfected with indicated combinations of NEMO and His-ubiquitin (His<sub>6</sub>-Ub) expression constructs and either treated with MG132 or left untreated, as indicated. (C) Diagram of experiments performed under denaturing conditions with metal chelation chromatography (Ni-NTA) to detect ubiquitylation *in vivo* in Fig. 5. (D)(*Top*) RT-PCR analysis of expression levels of Traf7 constructs in C2C12 cells. (*Bottom*) Western blot analysis after immunoprecipitation (IP) of lysates from confluent C2C12 cells expressing FLAG-Traf7 or RING mutant FLAG-Δ89-Traf7 indicates that both proteins interact with a common pool of NEMO with comparable efficiency. IP of 10 mg lysate with anti-FLAG beads. Immunoblots were probed with anti-NEMO and anti-FLAG antibodies (*top*), and

(bottom) input whole cell extract (WCE) was blotted with anti-NEMO and anti-tubulin (bottom) antibodies.

### Supplemental References

Acosta-Alvear D, Zhou Y, Blais A, Tsikitis M, Lents NH, Arias C, Lennon CJ, Kluger Y, Dynlacht BD (2007) XBP1 controls diverse cell type- and condition-specific transcriptional regulatory networks. *Molecular cell* **27**(1): 53-66

Asp P, Acosta-Alvear D, Tsikitis M, van Oevelen C, Dynlacht BD (2009) E2f3b plays an essential role in myogenic differentiation through isoform-specific gene regulation. *Genes & development* **23**(1): 37-53

Blais A, Tsikitis M, Acosta-Alvear D, Sharan R, Kluger Y, Dynlacht BD (2005) An initial blueprint for myogenic differentiation. *Genes & development* **19**(5): 553-569

Cao Y, Kumar RM, Penn BH, Berkes CA, Kooperberg C, Boyer LA, Young RA, Tapscott SJ (2006) Global and gene-specific analyses show distinct roles for Myod and Myog at a common set of promoters. *The EMBO journal* **25**(3): 502-511

Jüllig M, Zhang WV, Ferreira A, Stott NS. (2006) MG132 induced apoptosis is associated with p53-independent induction of pro-apoptotic Noxa and transcriptional activity of beta-catenin. *Apoptosis* **11**(4):627-41

Lauricella M, D'Anneo A, Giuliano M, Calvaruso G, Emanuele S, Vento R, Tesoriere G. (2003) Induction of apoptosis in human osteosarcoma Saos-2 cells by the proteasome inhibitor MG132 and the protective effect of pRb. *Cell Differentiation* **10**(8):930-932.

Lee TI, Jenner RG, Boyer LA, Guenther MG, Levine SS, Kumar RM, Chevalier B, Johnstone SE, Cole MF, Isono K, Koseki H, Fuchikami T, Abe K, Murray HL, Zucker JP, Yuan B, Bell GW, Herbolsheimer E, Hannett NM, Sun K, Odom DT, Otte AP, Volkert TL, Bartel DP, Melton DA, Gifford DK, Jaenisch R, Young RA (2006) Control of developmental regulators by Polycomb in human embryonic stem cells. *Cell* **125**(2): 301-313

Liu S, Spinner DS, Schmidt MM, Danielsson JA, Wang S, Schmidt J (2000) Interaction of MyoD family proteins with enhancers of acetylcholine receptor subunit genes in vivo. *The Journal of biological chemistry* **275**(52): 41364-41368

Ohno K, Sadeh M, Blatt I, Brengman JM, Engel AG (2003) E-box mutations in the RAPSN promoter region in eight cases with congenital myasthenic syndrome. *Human molecular genetics* **12**(7): 739-748



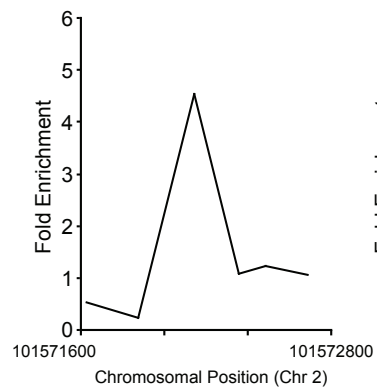
Spektor A, Tsang WY, Khoo D, Dynlacht BD (2007) Cep97 and CP110 suppress a cilia assembly program. *Cell* **130**(4): 678-690

Yoshiko Y, Hirao K, Maeda N (2002) Differentiation in C(2)C(12) myoblasts depends on the expression of endogenous IGFs and not serum depletion. *Am J Physiol Cell Physiol* **283**(4): C1278-1286

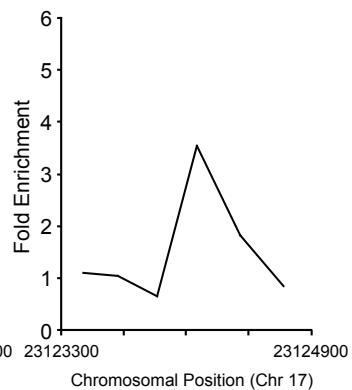
**MyoD1 targets associated with ubiquitin-related processes****(from individual and averaged ChIP-on-chip replicates and conventional ChIP assays)**

Gene ID	Gene Symbol	Gene Name	Gene Ontology (Molecular Function)
22225	Usp5	Ubiquitin specific peptidase 5	
252870	Usp7	Ubiquitin specific peptidase 7	
24110	Usp18	Ubiquitin specific peptidase 18	
54651	Usp27x	Ubiquitin specific peptidase 27, X chromosome	Cysteine-type ubiquitin hydrolase (deubiquitinating enzyme)
319651	Usp37	Ubiquitin specific peptidase 37	
28035	Usp39	Ubiquitin specific peptidase 39	
69727	Usp46	Ubiquitin specific peptidase 46	
381944	Dub1a	Deubiquitinating enzyme 1a	
74244	Atg7	Autophagy-related 7 (yeast)	
74153	Ube1l	Ubiquitin-activating enzyme E1-like	E1-like ubiquitin activating enzyme
22200	Uba3	Ubiquitin-like modifier activating enzyme 3	
66663	Uba5	Ubiquitin-like modifier activating enzyme 5	
22209	Ube2a	Ubiquitin-conjugating enzyme E2A, RAD6 homolog (S. cerevisiae)	E2 ubiquitin conjugating enzyme
70620	Ube2v2	Ubiquitin-conjugating enzyme E2 variant 2	
105193	Nhlrc1	NHL repeat containing 1	
66156	Anapc11	Anaphase promoting complex subunit 11	
69957	Cdc16	CDC16 cell division cycle 16 homolog (S. cerevisiae)	
100763	Ube3c	Ubiquitin protein ligase E3C	
29864	Rnf11	Ring finger protein 11	E3 ubiquitin-protein ligase, ubiquitin ligase activity
75841	Rnf139	Ring finger protein 139	
22034	Traf6	Tnf receptor-associated factor 6	
224619	Traf7	Tnf receptor-associated factor 7	
81003	Trim23	Tripartite motif-containing 23	
58522	Trim54	Tripartite motif containing 54 (muscle specific)	
230904	Fbxo2	F-box protein 2	
50755	Fbxo18	F-box protein 18	F-box protein, ubiquitin-protein ligase complex
67731	<b>Fbxo32</b>	<b>F-box protein 32 (X)</b>	
230903	Fbxo44	F-box protein 44	
19170	Psmb1	Proteasome (prosome, macropain) subunit, beta type 1	
26445	Psmb2	Proteasome (prosome, macropain) subunit, beta type 2	Integral component of the proteasome
19183	Psmc3ip	Proteasome (prosome, macropain) 26S subunit, ATPase 3, interacting protein	
66997	Psmc12	Proteasome (prosome, macropain) 26S subunit, non-ATPase, 12	
22218	Sumo1	SMT3 suppressor of mif two 3 homolog 1 (yeast)	Small ubiquitin-like modifier protein
66177	Ubl5	Ubiquitin-like 5	
223870	Senp1	SUMO/sentrin specific peptidase 1	Cysteine-type protease associated to the ubiquitin cycle
94092	<b>Trim16</b>	<b>Tripartite motif-containing 16 (X)</b>	
22670	Trim26	Tripartite motif-containing 26	Undetermined
360213	Trim46	Tripartite motif-containing 46	

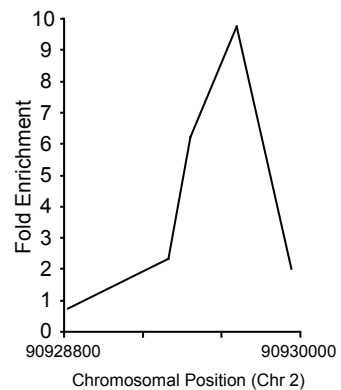
Fbxo32 and Trim16 marked with (X), were shown to be MyoD1 transcriptional targets in MEFs (Cao et al, 2006).



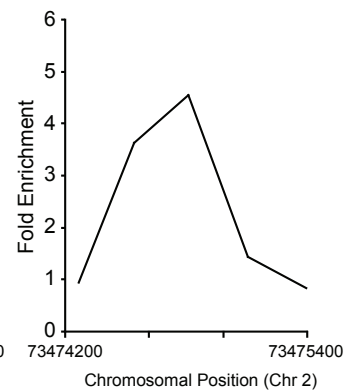
NM009424.2  
*Traf6* D84655  
 (Tnf receptor-associated factor 6)



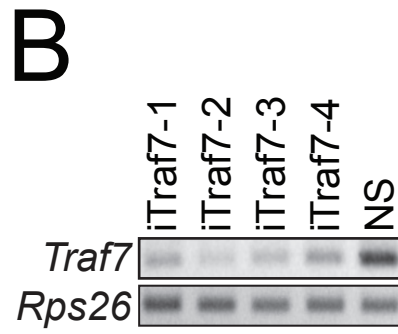
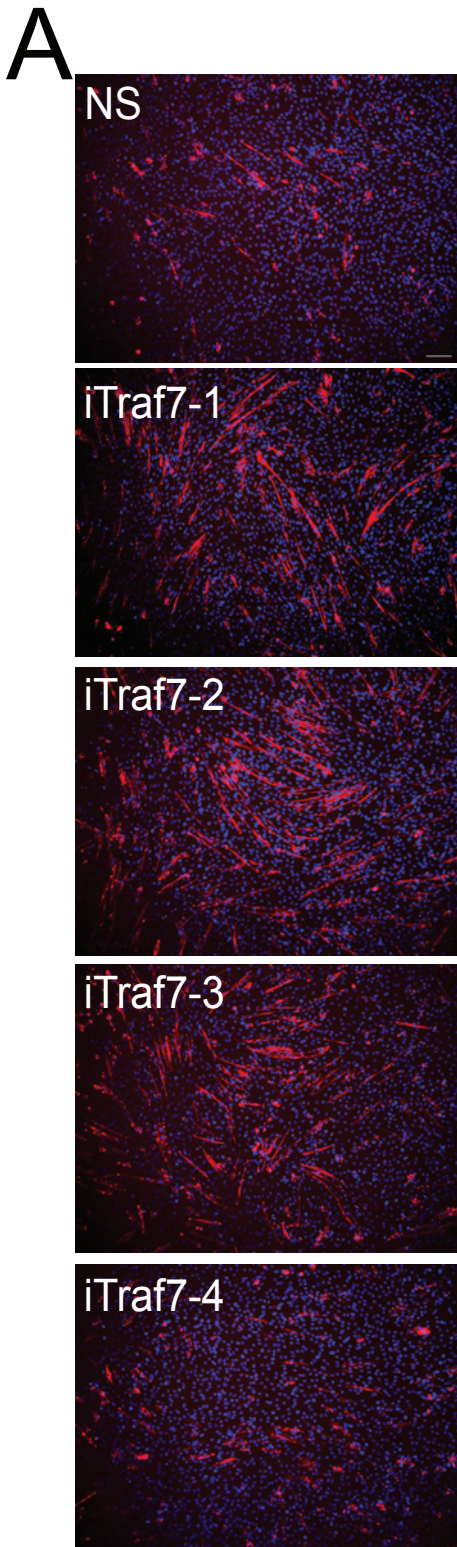
NM153792.1  
*Traf7*  
 (Tnf receptor-associated factor 7)



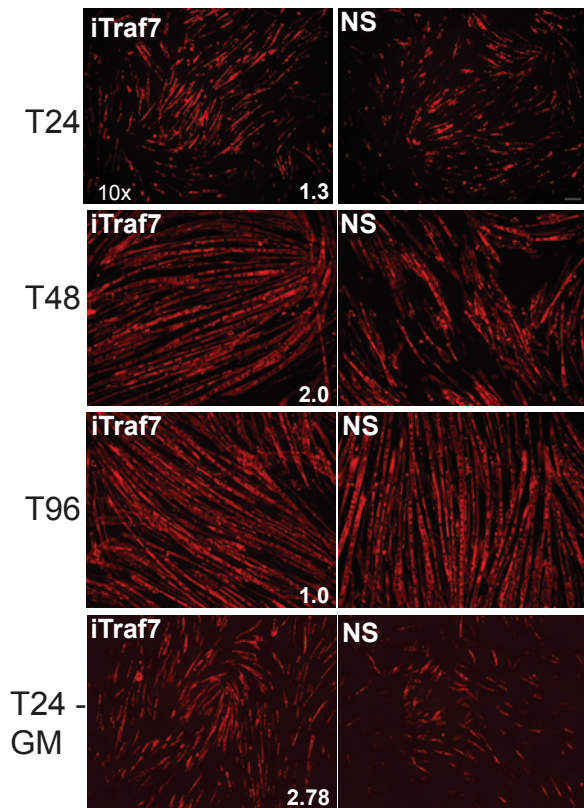
NM009023.2  
*Rapsn*  
 (Receptor-associated protein of the synapse)



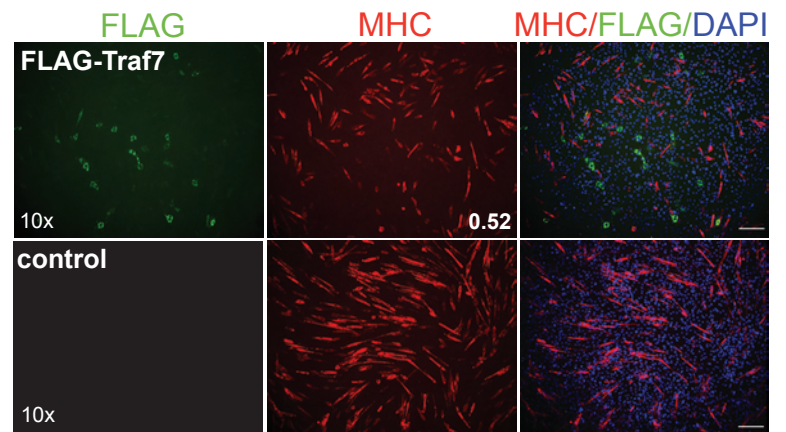
M17640  
 NM007389.4  
*Chrna1*  
 (Cholinergic receptor nicotinic alpha 1)



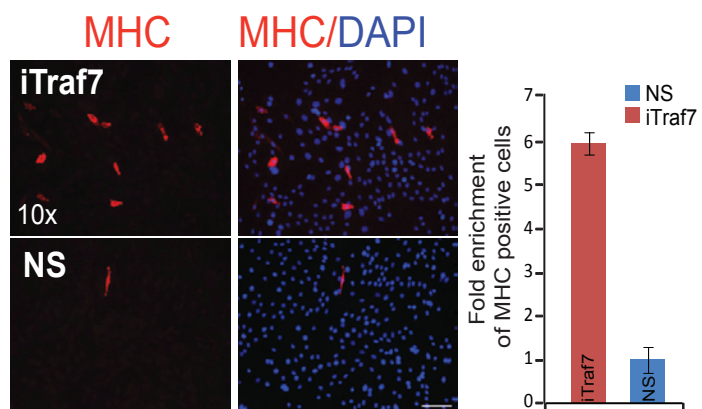
A



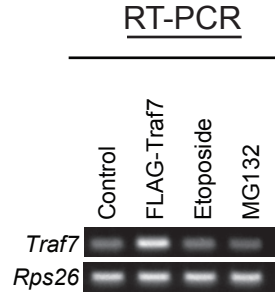
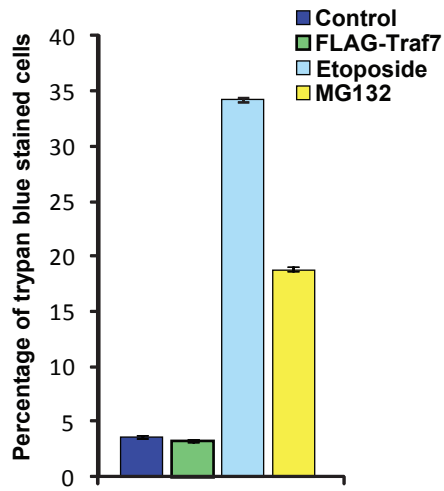
C



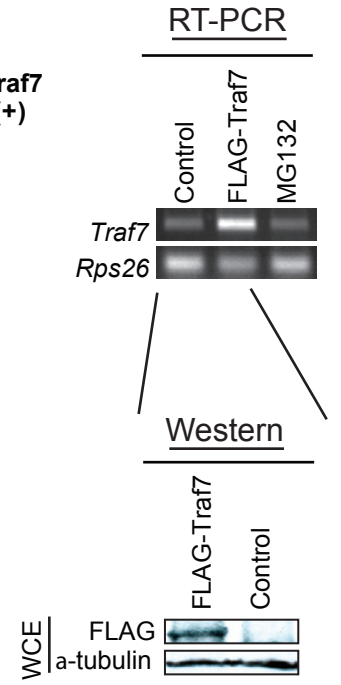
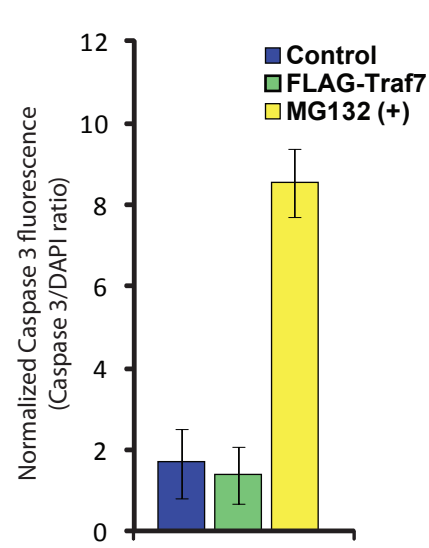
B



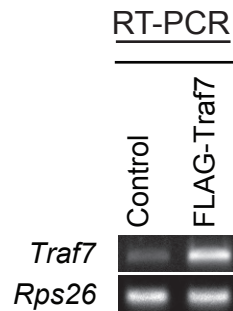
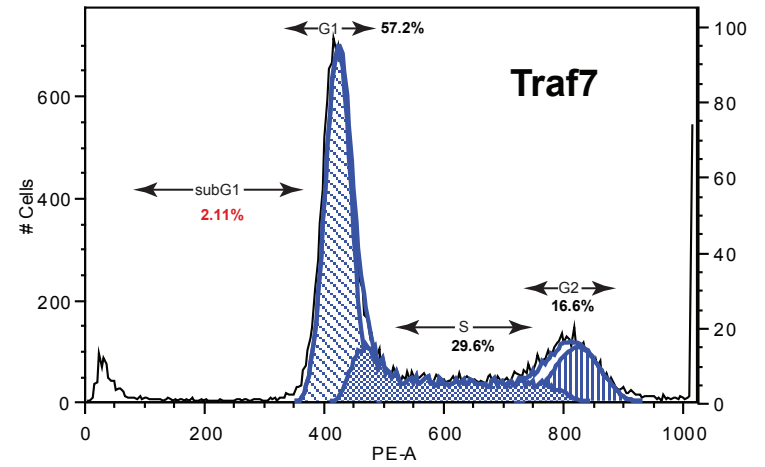
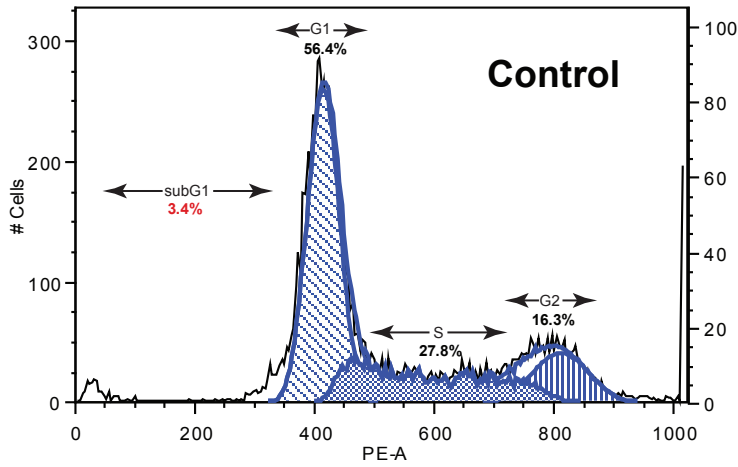
A)



B)

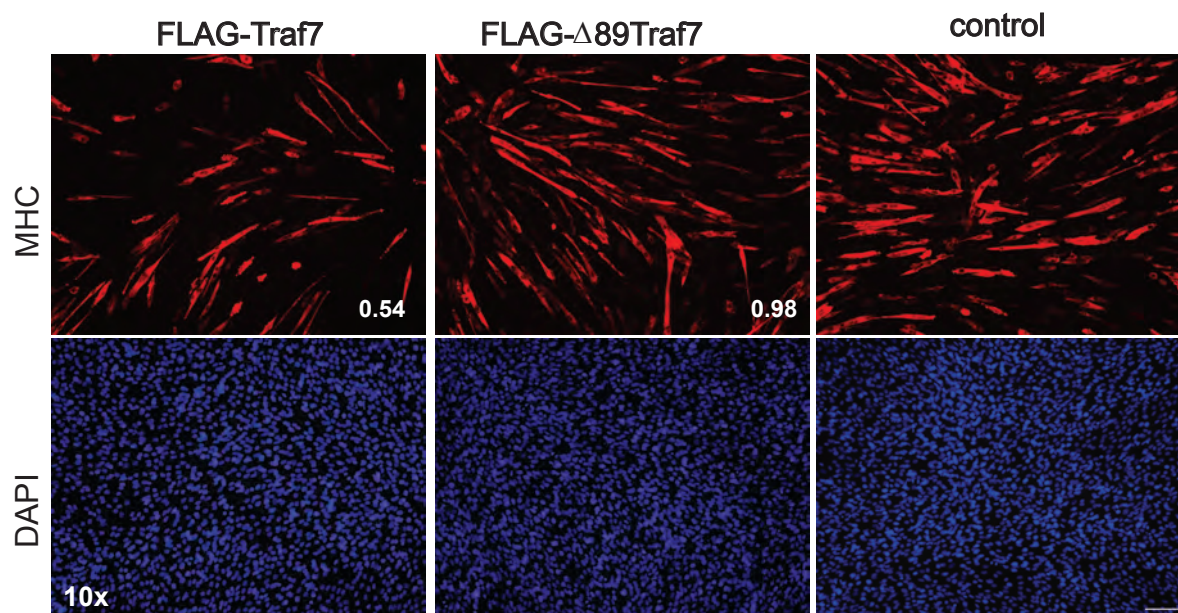


C)





A



B

